

## The Hydrolysis of Tert-Butylamine Borane By Using Ni-Zr-B-O Catalyst For Hydrogen Production

Hatice Begüm MURATHAN<sup>a</sup>, Göksel ÖZKAN<sup>b\*</sup>

<sup>a,b</sup>Department of Chemical Engineering, Gazi University, 06570 Maltepe, Ankara, Turkey

Email: gozkan@gazi.edu.tr

*Manuscript Received online 10/29/2020, Accepted 11/11/2020*

This study focuses on the catalytic hydrolysis of tert-butylamine borane (TBAB, C<sub>4</sub>H<sub>9</sub>NH<sub>2</sub>BH<sub>3</sub>) with Ni-Zr-B-O. For this aim, catalyst mixture was prepared by co-precipitation method using NaBH<sub>4</sub>. The effect of temperature and catalyst amount on the hydrolysis of TBAB was examined. It has been observed that for each catalyst amounts, an increase at the temperature significantly increases the hydrogen production yield and reduces the reaction time as well. Similar results were also observed in each catalyst amounts when the temperature was kept constant. The maximum yield of the hydrogen production was found as 2.94 mol H<sub>2</sub>/mol TBAB (98%) at 55°C temperature, having 0.05 g catalysis in 656 seconds. Reaction enthalpy ( $\Delta H^{++}$ ) and entropy ( $\Delta S^{++}$ ) and turnover frequency value were calculated as 46.06 kJ.mol<sup>-1</sup> -189.05 J.mol<sup>-1</sup>.K<sup>-1</sup> and 789 mol H<sub>2</sub>.mol Ni<sup>-1</sup>.min<sup>-1</sup> respectively. Finally, catalyst characterization was done by XRD and XPS and Ni average crystalline size was found as 29.8 nm from Scherrer equation.

Keywords: tert-Butylamine Borane, Hydrogen Storage, Hydrolysis, Dehydrogenation

### Introduction

A significant portion of the energy needed today is provided from carbon-based fossil fuels which are limited and non-environmental. Renewable energy sources such as solar energy, and wind energy provide small portion of energy supply where the batteries and super capacitors are used as storage for sustainability. Recently, one of the other approaches' is using hydrogen as an energy carrier<sup>1-5</sup>.

Hydrogen is a well-known green energy and plays an important role in sustainable energy. Several types of studies are focused on hydrogen production, storage, safety, utilization and economy. Physicals like carbon based nanotubes, metal organic frameworks or chemicals like ammonia, methanol, borohydrides, amine boranes are

well-known for storing hydrogen. In boron based chemicals researchers mostly use borohydrides. Amine boranes are also used as an alternative of borohydrides for hydrogen storage material. The most studied material is ammonia borane (basic of amine boranes) a widely known H<sub>2</sub> storage material. Owing to ammonia boranes theoretically high H<sub>2</sub> content, being stable and non-toxic structure, it can be used as hydrogen storage material for fuel cell applications<sup>2, 6-10</sup>. The dehydrogenation of the amine boranes is generally carried out by catalytic or non-catalytic hydrolysis, thermolysis or methanolysis<sup>11-13</sup>. RuCl<sub>3</sub>, RhCl<sub>3</sub>, PdCl<sub>2</sub>, CoCl<sub>2</sub>, NiCl<sub>2</sub>, Pd/C, and Raney-Ni were the first catalyst types that were reported for catalytic hydrolysis of amine boranes at low temperatures<sup>14</sup>. Various support materials such as graphene oxide, TiO<sub>2</sub>, activated carbon, and

alumina are used on the catalyst. Ru, Rh, Pd are used as the coating of support materials by impregnation method. In addition, cheaper materials such as Co, Cu and Ni are used<sup>15-21</sup>. Similar to catalytic hydrolysis, catalytic methanolysis is carried out at low temperatures. Thermolysis of ammonia borane releases 3 moles of H<sub>2</sub> in different temperature ranges (110-500°C). During dehydrogenation of ammonia borane, trace amounts of byproducts such as ammonia (NH<sub>3</sub>), and diborane (B<sub>2</sub>H<sub>6</sub>) may cause catalyst poisoning. One of the approaches used to avoid poisoning was using alkyl or aryl amine boranes. Low carbon alkyl amine boranes like methylamine borane and dimethylamine borane were hydrolyzed for hydrogen generation<sup>22-24</sup>. At the end of hydrolysis, these low carbon alkyl amines are formed into gases which affect the impurity of hydrogen. However, tert-butylamine is suitable because at the end of hydrolysis this material stays as liquid which does not change the purity of hydrogen. Moreover, having an alkyl group in the structure accelerates the release of hydrogen compared to ammonia borane. In many studies, hydrolysis reaction of amine boranes was used for in-situ catalyst preparation. Due to their Lewis structure, these compounds are suitable for hydrogen production by catalytic dehydrogenation. Tert-butylamine borane (TBAB, 16wt% H<sub>2</sub>) like any other amine boranes is already well known as a reduction agent for various substances. Thermolysis of tert-butylamine borane conducted close to the melting point (90-95°C), releases hydrogen, polyimido-boranes ((BNH)<sub>n</sub> and (CBNH)<sub>n</sub>) according to MAS-NMR and thermo gravimetric analyses. These by-products could be used as a good regeneration path<sup>25-27</sup>.

In this study, catalytic hydrolysis of TBAB was examined. Ni-Zr-B-O catalyst was prepared by co-precipitation method with NaBH<sub>4</sub> containing 40% Ni and 60% Zr by mass and analyzed by X-Ray Diffraction (XRD) and X-Ray Photoelectron Spectroscopy (XPS). Catalyst amount (0.0025g and 0.05g) and temperature (30°C, 40°C and 55°C) effect on hydrolysis were investigated. Kinetic studies were applied. E<sub>a</sub>, ΔH<sup>++</sup> and ΔS<sup>++</sup> were calculated.

## **Experimental**

### *(A) Materials*

Tert-butylamine borane (C<sub>4</sub>H<sub>9</sub>NH<sub>2</sub>BH<sub>3</sub>, Sigma), nickel (II) chloride hexahydrate (NiCl<sub>2</sub>·6H<sub>2</sub>O, Aldrich), zirconium (IV) chloride (ZrCl<sub>4</sub>, Aldrich), sodium borohydride (NaBH<sub>4</sub>, Fluka) and deionized water were used.

### *(B) Preparation of Ni-Zr-B-O Catalyst*

The mixture of 0.059M nickel chloride hexahydrate and 0.065M zirconium chloride, 0.18 M sodium borohydride was added in droplets and homogeneously dispersed by magnetic stirrer in ice-water bath. The precipitate was separated by centrifuge, washed 4 times using deionized hot water to separate from impurities and finally left to dry at 105°C.

### *(C) Characterization of Catalyst*

Phase structures of the catalyst were analyzed by XRD analysis (the PANalytical brand Empyrean), using copper (Cu) tube between 5-90°, operating at 45 mA and 40 kV. The electronic states of the catalyst surface were examined XPS (Thermo Scientific / K-Alpha Brand XPS Device).

### *(D) Catalytic Hydrolysis of TBAB*

Hydrolysis of 0.2% by weight aqueous solution of tert-butylamine borane was performed at 30°C, 40°C and 55°C having two different catalyst amounts (0.0025g and

0.05g). Batch reaction system is given in Fig. 1. System contains 50 ml volume 2 neck glass reactor, 50 ml volume pressure stabilizing liquid feeding apparatus and washing bottle having 0.1M H<sub>2</sub>SO<sub>4</sub> solution. The produced hydrogen was measured as function of time in a 250 ml gas burette system.

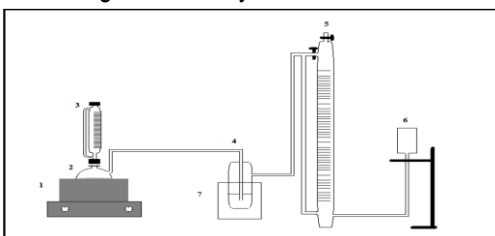


**Fig. 1.** Batch reaction system experimental setup, ((1) heater-magnetic stir plate, (2) batch reactor, (3) TBAB-water solution, (4) wash bottle, (5) gas burette system (6) drip funnel (7) cold water bath)

## Results and discussion

### (A) Catalyst characterization

XRD analysis of Ni-Zr-B-O catalyst is given in Fig.2. The non used catalyst is found to be crystalline (Isometric - Hexoctahedral) Ni at angles of 44.72°; 51.99°; 76.49°. Ni average crystalline size was calculated by using Scherrer equation (Eq. 1):

$$D = \frac{k\lambda}{\beta \cos \theta} \quad (1)$$

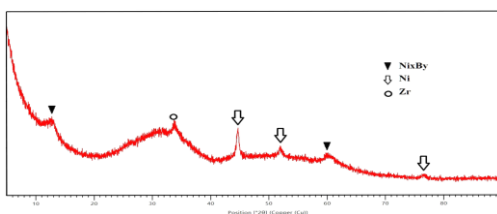


**Fig. 2.** XRD result of Ni-Zr-B-O

where, D is grain/crystallite size, k is shape factor (0.9),  $\lambda$  is X-ray wavelength,  $\beta$  is the line broadening at half the maximum intensity in radians (FWHM) and the  $\theta$  is the Bragg angle. Ni average crystallite size was calculated as 29.8nm. The structure contains Ni<sub>x</sub>B<sub>y</sub> observed

at 12.67° and 60.03°. Also semi-amorphous form of Zr is observed between 23-40°. Broad peaks around the 30° is found to be amorphous Zr(OH)<sub>4</sub> which is good agreement in previous studies<sup>28,29</sup>.

Fig. 3 shows the B, Ni, O and Zr XPS spectra of the catalyst. Peak of B1s having an electron binding energy at 191.78 eV shows oxidized boron. At 874.88 eV region of Ni 2p<sub>1/2</sub> peak was observed which represents Ni(0). From peaks of Ni2p and O1s having an electron binding energy at 855.51 eV and 531.19 eV belong oxidized Ni. On the Zr 3d spectra of the sample, the peaks at 181.3 eV and 184.58 eV can be assigned to the Zr 3d<sub>5/2</sub> and Zr 3d<sub>3/2</sub> binding energy levels.

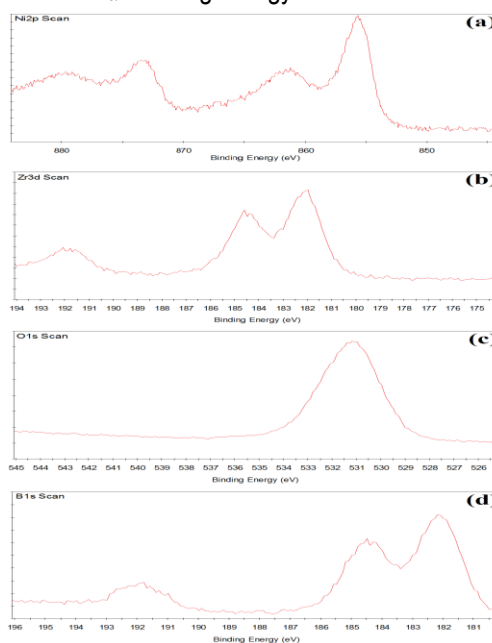


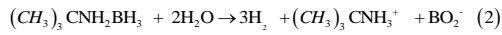
**Fig. 3.** XPS results of Ni-Zr-B-O (a) Ni 2p (b) Zr 3d (c)O1s and (d) B1 scans

The standard value of the Zr3d<sub>5/2</sub> peak is at 182.2 eV and the binding state level represents amorphous/hydrous zirconia (ZrO<sub>2</sub>nH<sub>2</sub>O) according to previous studies<sup>29-33</sup>. However, when compared with this study, zirconium is in the oxide state similar to the nickel. This is due to the preparation conditions where the

catalysts were produced in aqueous dilute solution.  $\text{Ni}^{2+}$  was reduced to  $\text{Ni}(0)$  by  $\text{NaBH}_4$ , and nickel boride and  $\text{Ni}(\text{OH})_2$  were also formed. Zr was not reduced but oxidized where the catalyst was not exposed to any heat above  $105^\circ\text{C}$  in preparation steps. In order to form Zr oxide, product must be heated above  $700^\circ\text{C}$ <sup>28</sup>. So mostly Zr was in the form of  $\text{Zr}(\text{OH})_4$ .

#### (B) Catalytic Hydrolysis Results of TBAB

Catalytic hydrolysis of TBAB was studied with Ni-Zr-B-O catalyst. Temperature ( $30^\circ\text{C}$ ,  $40^\circ\text{C}$  and  $55^\circ\text{C}$ ) and the amount of catalyst effect (0.0025g, and 0.05g) were studied. At the end of TBAB hydrolysis 3 mol of hydrogen was released from borane part (Eq. 2).



In Fig. 4, when the catalyst amount was 0.0025g and the temperature was between  $30^\circ\text{C}$  and  $55^\circ\text{C}$ , reaction time shortened (3000s to 720s) and hydrogen production increased (2.2 to 2.72 mol  $\text{H}_2/\text{mol}$   $\text{TBAB}_0$ ) respectively. When the amount of catalyst was increased to 0.05g, mol ratios of  $n\text{H}_2/n\text{TBAB}_0$  were achieved 2.77 at 3130s, 2.94 at 656s for temperatures  $30^\circ\text{C}$  and  $55^\circ\text{C}$  respectively. Clearly for both catalyst amounts, an increase in temperature significantly increased the hydrogen production yield and reduced the reaction time. The same effect was also observed for the catalyst amount. Ruthenium is one of the best active side on hydrolysis reaction of amine boranes given in literature<sup>14</sup>. However, using nickel is less expensive and can be well effective according to these results. Akbayrak et. al. used Ni (95wt.%) activated carbon catalyst for the hydrolysis of ammonia borane at room temperature in 30min and achieved a result that was close to 100% yield  $\text{H}_2$  production<sup>34</sup>. In this study, 98%

efficiency was obtained with Ni-Zr-B-O catalyst in 50min reaction time at  $30^\circ\text{C}$ . When compared with the literature, using Ni-Zr-B-O catalyst provided high efficiency (98%), however reaction time can be reduced by either variables; increasing the amount of nickel or increasing the temperature.

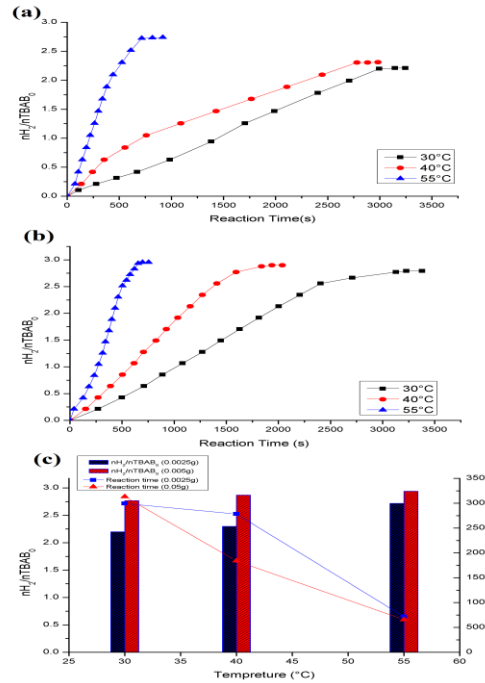


**Fig. 4.** Hydrolysis of 0.2% TBAB in the presence of Ni-Zr-B-O catalyst; (a) 0.0025g cat., (b) 0.05g cat., (c)  $n\text{H}_2/n\text{TBAB}_0$ -Temperature-Reaction Time graph

Kinetic results of TBAB hydrolysis with Ni-Zr-B-O catalyst were given in Fig. 5. Reaction rate was found as a zero order which was suitable for exponential kinetics. Most of amine borane catalytic solvolysis reactions are zero or first order<sup>10</sup>. Activation energy was calculated by Arrhenius equation (Eq. 3):

$$\ln k = \ln k_0 - (E_a/RT) \quad (3)$$

where the  $k_0$  is frequency constant,  $E_a$  is activation energy,  $R$  is gas constant and  $T$  is temperature. From the plot of Arrhenius (Fig 5b), activation energy was determined as 48.68 kJ.mol<sup>-1</sup>. Table 1 shows the comparison of  $E_a$  of different catalysts. Reaction enthalpy and entropy were calculated according to Eyring equation (Eq 4):

$$\ln\left(\frac{k}{T}\right) = \ln\left(\frac{k_B}{h}\right) + \left(\frac{\Delta S^\ddagger}{R}\right) - \left(\frac{\Delta H^\ddagger}{R}\right)\left(\frac{1}{T}\right) \quad (4)$$

where  $h$  is Planck's constant and  $k_B$  is Boltzman constant. From plot of Eyring (Fig. 5c), reaction enthalpy and entropy were calculated as 46.06 kJ.mol<sup>-1</sup> and -189.05 J.mol<sup>-1</sup>.K<sup>-1</sup> respectively. Turnover frequency value was found as 789 mol H<sub>2</sub>.mol Ni<sup>-1</sup>.min<sup>-1</sup> at 55°C.

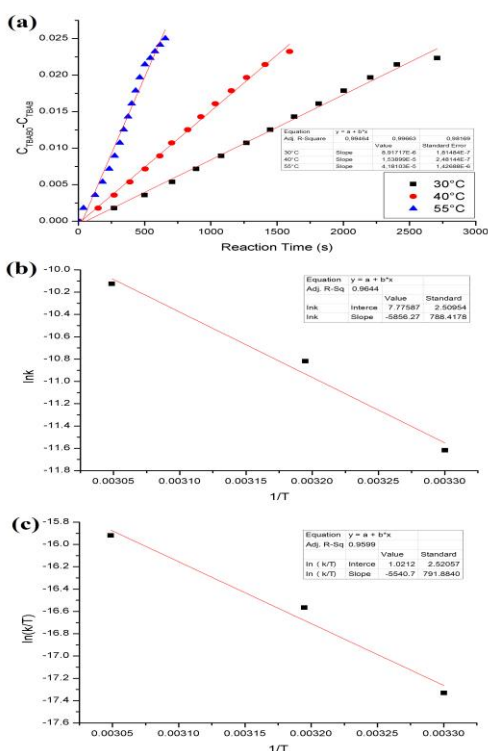


**Fig. 5.** Kinetic results for Ni-Zr- B-O catalyst (a)  $C_{TBAB0}-C_{TBAB}$  versus time graphs (b)  $\ln(k)$  versus  $1/T$  plot, (c)  $\ln(k/T)$  versus  $1/T$  plot

**Table 1.** Dehydrogenation of amine boranes with different catalyst activation energies

Catalyst	Amine Borane	$E_a$ (kJ/mol)	Ref.
Ru/graphene NPs	AB*	11	35
Ru/Al <sub>2</sub> O <sub>3</sub>	AB	23	36
Ni <sub>0.75</sub> B <sub>0.25</sub>	AB	44.16	37
Ni <sub>2</sub> P NPs	AB	44.6	38
Ru/Al <sub>2</sub> O <sub>3</sub>	AB	48	39
Ni-Zr-B-O	TBAB	48.68	this work
Cu <sub>0.75</sub> B <sub>0.25</sub>	AB	50.77	37
Pd-PVB-TiO <sub>2</sub>	AB	56	40

\*AB means ammonia borane

## Conclusions

Catalytic hydrolysis of TBAB with Ni-Zr-B-O was carried out. The effect of temperature and catalyst amount was examined. Hydrogen production yield was increased by increasing the temperature or catalyst amount. Moreover, the reaction time was also reduced. Highest hydrogen yield was observed as 98% at 656s where the temperature and catalyst amount were 55°C and 0.05g respectively. Activation energy was calculated as 48.68 kJ.mol<sup>-1</sup>.  $\Delta H^\ddagger$  and  $\Delta S^\ddagger$  were determined as 46.06 kJ.mol<sup>-1</sup> and -189.05 J.mol<sup>-1</sup>.K<sup>-1</sup>. Turnover frequency value was computed as 789 mol H<sub>2</sub>.mol Ni<sup>-1</sup>.min<sup>-1</sup> at 55°C.

## Acknowledgements

The authors appreciate the financial support from the Gazi University Projects of Scientific Investigation (BAP) within the project "06/2018-08".

## References

1. Y. S. Najjar, *I.J. of Hyd. En.*, 2013, **38**(25), 10716-10728.
2. A. Züttel, *Naturwissenschaften*, 2004, **91**.4: 157-172.
3. N. L. Panwar, S. C. Kaushik, S. Kothari, *Renew. and Sust. En. Rev.*, 2011, **15**.3:1513-1524.

4. P. A. Owusu, S. Asumadu-Sarkodie, *Cogent Eng.*, 2016, **3**(1): 1167990.
5. A. González, E. Goikolea, J. A. Barrena, R. Mysyk, *Renew. and Sust. En. Rev.*, 2016, 58: 1189-1206.
6. M.Yadav, Q. Xu, *En. and Envir. Sci.*, 2012, 5(12), 9698-9725.
7. N. E. Stubbs, A. P. Robertson, E. M. Leitao, I. Manners, *J.I of Organometallic Chem.*, 2012, **730**, 84-89.
8. H. Li, Q. Yang, X. Chen, S. G. Shore, *J. of Organometallic Chem.*, 2014, **751**, 60-66.
9. Z.Ozturk, D. A. Kose, Z. S. Sahin, Z. G. Ozkan, A. Asan, *Int. J. of Hyd. En.*, 2016, **41**(28), 12167-12174.7.
10. S. Kumar, T. J. D. Kumar, *J. Indian Chem. Soc.*, 2019, **96**, 793-800.
11. H. Chu, N. Li, S. Qiu, Y. Zou, C. Xiang, F. Xu, L. Sun, *I. J. of Hyd. En.*, 2019, **44**(3), 1774-1781.
12. H. B. Murathan, G. Özkan, M. S. Akkuş, D. Ö. Özgür, G. Özkan, *I. J. of Hyd. En.*, 2018, **43**(23), 10728-10733.
13. J. F. Petit, U. B. Demirci, *Int. J. of Hyd. En.*, 2019, **44**(27), 14201-14206.
14. P. V. Ramachandran, P. D. Gagare, *Inorganic Chem.*, 2007, **46**(19), 7810-7817.
15. M. Rakap, *J. of Alloys and Compounds*, 2015, **649**, 1025-1030
16. D: Ö. Özgür, T. Şimşek, G. Özkan, M. S. Akkuş, G. Özkan, *Int. J. of Hyd. En.*, 2018, **43**(23), 10765-10772.
17. X. Chen, X. J. Xu, X. C. Zheng, X. X. Guan, P. Liu, *Mat. Res. Bulletin*, 2018, **103**, 89-95.
18. F. Zhang, C. Ma, Y. Zhang, H. Li, D. Fu, X. Du, X. M. Zhang, *J. of P. Sources*, 2018, **399**, 89-97.
19. L. X. Xu, L. N. Yang, L. H. Shang, J. R. Chen, In *IOP Conference Series: Mat. Sci. and Eng.*, 2018, **382**, 2, 022097.
20. A. Yousef, N. A. Barakat, M. H. El-Newehy, M. M. Ahmed, H. Y. Kim, H. Y. *Colloids and Surfaces A: Physicochemical and Eng. Asp.*, 2015, **470**, 194-201.
21. N. Cao, J. Su, W. Luo, G. Cheng, *G. Cat. Com.*, 2014, **43**, 47-51.
22. S. Basu, Y. Zheng, J. P. Gore, *J. of P. Sources*, 2011, **196**(2), 734-740.
23. S. Taçyıldız, B. Demirkan, Y. Karataş, M. Gülcan, F. Şen, *J. of Molecular Liq.*, 2019, **285**, 1-8.
24. Y. Chen, J. L. Fulton, J. C. Linehan, T. Autrey, *J. of the Amer. Chm.I Soc.*, 2005, **127**(10), 3254-3255.
25. J.Feigerle, N. Smyrl, J. Morrell, A. C. Stowe, In *Mat. Ch. in Alt. and Renew. En., Ceramic Transaction* (G. Wicks, at al.), *John Wiley & Sons, Inc.* 2010, **224**, 73-80.
26. D. Kundu, S. Chakma, G. Pugazhenth, T. Banerjee, *T. ACS omega*, 2018, **3**(2): 2273-2281.
27. P. Bellham, M. S. Hill, G. Kociok-Kohn, *Organometallics*, 2014, **33**(20), 5716-5721.
28. M. Aghazadeh, A. A. M. Barmi, M. Hosseinifard, *Mat. Let.*, 2012, **73**, 28-31.
29. Q. Liu, X. Dong, Y. Song, W. Lin, *J. of Natural Gas Chem.*, 2009, **18**(2), 173-178.
30. N. Tunç, M. Rakap, *Renew. En.*, 2020, **155**, 1222-1230.
31. Q. Yang, W. Yuan, X. Liu, Y. Zheng, Z. Cui, X. Yang, S. Wu, *Acta Biomaterialia*, 2017, **58**, 515-526.
32. C. Huang, Z. Tang, Z. Zhang, *J. of the Amer. Cer. Soc.*, 2001, **84**(7), 1637-1638.
33. X. Cai, Q. Xu, G. Tu, Y. Fu, F. Zhang, W. Zhu, *Frontiers in Chem.*, 2019, **7**, 42.
34. S. Akbayrak, Z. Özçifçi, A. Tabak, *Biomass and Bioen.*, 2020, **138**, 105589.
35. N. Cao, W. Luo, G. Cheng, *I. J. Hyd. En.*, 2013, **38**, 11964-11972.
36. M. Chandra, Q. Xu, *J. Power Sources*, 2007, **168**, 135-142.
37. A. K. Figen *Int.I J.Hyd. En.*, 2013, **38**(22), 9186-9197.
38. C. Peng, L. Kang, S. Cao, Y. Chen, Z. Lin, W. Fu, *Angew Chem Int Ed* 2015, **54**, 15725-15729.
39. H. Can, O. Metin, *App. Cat. B Envir.* 2012, **125**, 304-310.

40. M. Rakap, E.W. Kalu, S. Özkar, *Int. J. Hyd. En.*, 2011, **36**, 1448–1455.